Cell Reports

PD-1 Is Involved in the Dysregulation of Type 2 Innate Lymphoid Cells in a Murine Model of Obesity

Graphical Abstract

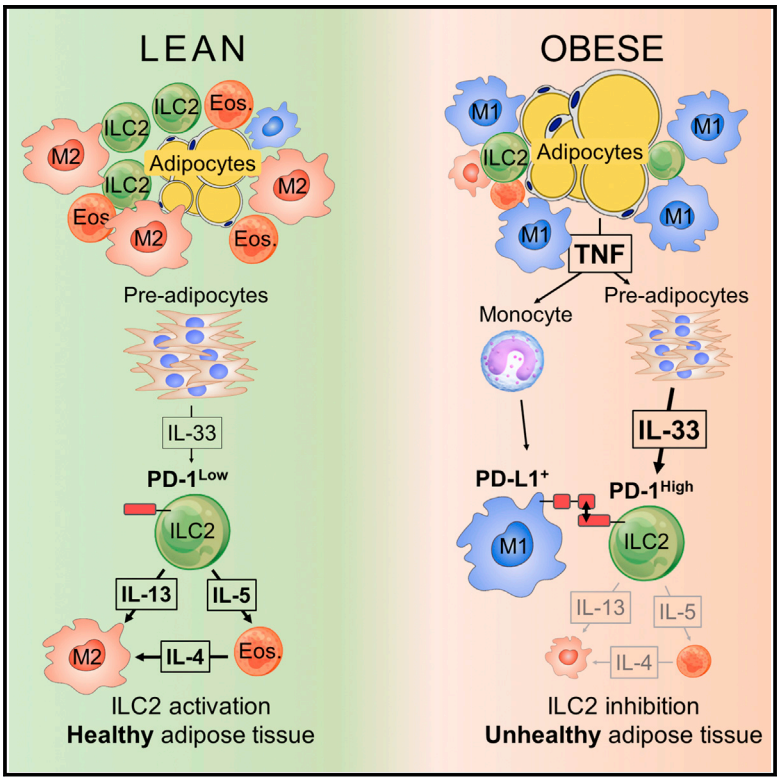

Highlights

- PD-1 is upregulated on ILC2s in adipose tissue of obese mice
- PD-1 expression is increased in a TNF- and IL-33-dependent manner
- PD-1 correlates with impaired ILC2 function in the presence of PD-L1^{+} macrophages
- PD-1 blockade ameliorates glucose tolerance and adaptation to environmental cold

Authors

Guillaume Oldenhove, Elodie Boucquey, Anaelle Taquin, ..., Kevin Englebert, Louis Boon, Muriel Moser

Correspondence

guillaume.oldenhove@ulb.ac.be

In Brief

The function of ILC2s is compromised during obesity. Here, Oldenhove et al. show that ILC2 inhibition is mediated by the PD-1-PD-L1 pathway. PD-1 blockade in obese mice improved ILC2 function, reinforced type 2 innate responses, and promoted tissue homeostasis. PD-1 may therefore represent a target for immune intervention in obesity-associated disorders.

Oldenhove et al., 2018, Cell Reports *25*, 2053–2060
November 20, 2018
https://doi.org/10.1016/j.celrep.2018.10.091

CellPress

Cell Reports
Report

PD-1 Is Involved in the Dysregulation of Type 2 Innate Lymphoid Cells in a Murine Model of Obesity

Guillaume Oldenhove,[1,4,*] Elodie Boucquey,[1] Anaelle Taquin,[1] Valérie Acolty,[1] Lynn Bonetti,[1] Bernhard Ryffel,[2] Marc Le Bert,[2] Kevin Englebert,[1] Louis Boon,[3] and Muriel Moser[1]
[1]Laboratory of Immunobiology, Department of Molecular Biology, Université Libre de Bruxelles, 6041 Gosselies, Belgium
[2]INEM, UMR7355, Molecular Immunology, University and CNRS, 40571 Orléans, France
[3]Bioceros, Yalelaan 46, 3584 CM Utrecht, the Netherlands
[4]Lead Contact
*Correspondence: guillaume.oldenhove@ulb.ac.be
https://doi.org/10.1016/j.celrep.2018.10.091

SUMMARY

Recent observations clearly highlight the critical role of type 2 innate lymphoid cells in maintaining the homeostasis of adipose tissues in humans and mice. This cell population promotes beiging and limits adiposity directly and indirectly by sustaining a Th2-prone environment enriched in eosinophils and alternatively activated macrophages. Accordingly, the number and function of type 2 innate lymphoid cells (ILC2s) are strongly impaired in obese individuals. In this work, we identify the PD-1-PD-L1 pathway as a factor leading to ILC2 destabilization upon high-fat feeding resulting in impaired tissue metabolism. Tumor necrosis factor (TNF) appears to play a central role, triggering interleukin-33 (IL-33)-dependent PD-1 expression on ILC2s and recruiting and activating PD-L1^{hi} M1 macrophages. PD-1 blockade partially restores the type 2 innate axis, raising the possibility of restoring tissue homeostasis.

INTRODUCTION

There is increasing evidence that immune parameters are profoundly deregulated in obese individuals, creating a state of inflammation that affects the homeostasis of multiple tissues and leads to metabolic disorders, such as diabetes and cardiovascular disease (Kanneganti and Dixit, 2012).

A number of recent reports have clearly identified the interleukin-33 (IL-33)/type 2 innate lymphoid cell (ILC2) axis (an IL-1 family member and its receptor; Neill et al., 2010) as a major regulator of adiposity. Indeed, adipose-tissue-resident ILC2s regulate the number and function of eosinophils and alternatively activated macrophages, ultimately preserving tissue metabolic homeostasis (Molofsky et al., 2013). ILC2s have been shown to promote the beiging of white adipose tissue directly through methionine enkephalin peptides as well as indirectly by sustaining norepinephrine and IL-4 producers (i.e., macrophages and eosinophils) (Brestoff et al., 2015; Qiu et al., 2014; Wolf et al., 2017a), and dysregulated ILC2 responses have been associated with obesity in mice and humans (Brestoff et al., 2015). Therefore, the identification of the factors leading to the disruption of ILC2 homeostasis appears critical, as they may constitute a powerful target for immunointervention.

Mechanistically, the loss of ILC2s in obese animals could result from the conversion of ILC2s into functionally distinct ILCs or from a counter-regulatory mechanism initiated by inflammatory cytokines. Indeed, the high degree of plasticity common to all ILC populations renders these cells highly sensitive to environmental clues, leading to transdifferentiation of ILC2s into ILC1 or ILC3 (Lim et al., 2016; Moro et al., 2016). Alternatively, ILC2 function may be repressed in the adipose tissue of obese mice. Studies by Molofsky et al. (2015) indicated that interferon γ (IFN-γ)-producing lymphocytes accumulated in the visceral adipose tissue (VAT) in response to a high-fat diet and could repress the maintenance of activated ILC2s in various settings. Another report demonstrated increased insulin sensitivity and decreased adipocyte size in obese IFN-γ knockout (KO) mice compared to obese wild-type (WT) mice, despite similar body weights (O'Rourke et al., 2012). The objective of this work was to analyze the very first step of the chronic inflammatory response leading to the loss of ILC2 function in mice fed a high-fat diet in order to identify the cellular and molecular mechanisms involved in the disruption of ILC2 homeostasis.

RESULTS

TNF Is Involved in ILC2 Dysregulation and PD-1 Upregulation in HFD-Fed Mice

We examined various cell populations of the type 2 innate immune responses in a murine model of obesity. Male mice were placed on a high-fat diet (HFD) starting at 8 weeks of age and gained 60%–100% of weight within 10–12 weeks compared to control mice (Figure 1A). The proportion of ILC2s in the adipose tissue, as well as the absolute numbers of ILC2s expressing IL-13, M2-type macrophages, and eosinophils were strongly reduced at 20 weeks of age (Figure S1A). These observations confirmed published reports showing that ILC2s are resident in fat, promote accumulation of eosinophils and M2-type macrophages, and collapse in mice fed an HFD (Brestoff et al., 2015; Molofsky et al., 2015). Comparison of cellular infiltrates in ILC-deficient (RAG γc KO) versus sufficient (RAG KO) mice

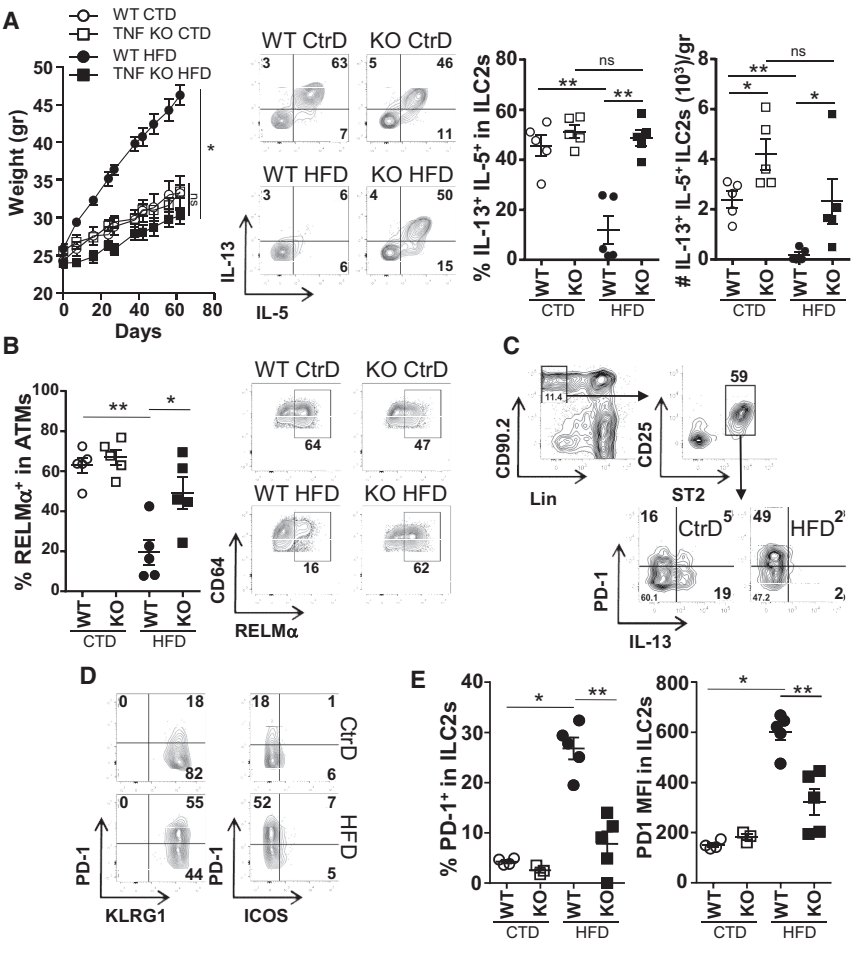

Figure 1. Increased PD-1 Expression Correlates with Decreased ILC2 Function during Obesity

(A) Body weight of control and high-fat diet (HFD)-fed wild-type (WT) and TNF KO mice and IL-5 and IL-13 expression (frequency and absolute number per gram of fat) in ILC2s from the same mice stimulated shortly *in vitro* with phorbol myristate acetate (PMA)-ionomycin in the presence of brefeldin A.

(B) Proportion of CD64$^+$ adipose tissue macrophages (ATMs) expressing RELMα from control and HFD-fed WT and TNF KO mice.

(C) Gating strategy and proportion of ILC2s expressing PD-1 and IL-13 in control and HFD-fed mice.

(D) PD-1, KLRG1, and ICOS expression in ILC2s from control and HFD-fed mice (1 individual mouse representative of 5).

(E) Frequency of PD1$^+$ cells among ILC2s and intensity of PD-1 expression (MFI) from control and HFD-fed WT and KO mice.

Error bars represent the SD of the mean (n = 3–5 mice per group). A non-parametric Mann-Whitney *U* test was used to determine statistical differences (*p < 0.05; **p < 0.01; ns, not significant). Data are representative of 3 independent experiments.

confirmed the prominent role of ILCs in eosinophil recruitment in mice fed a standard diet (Figure S1B).

We first tested whether the loss of ILC2s resulted from their transdifferentiation into ILC1 or ILC3s. The comparison of cell populations in the adipose tissue of mice under standard or high-fat feeding clearly showed that ST2$^+$ ILC2s (identified as CD90.2$^+$Lin$^-$CD25$^+$Sca1$^+$IL-33R$^+$) did not gain expression of T-bet or RORγt, and maintained their expression of GATA-3 and ST2 (Figure S2). These data suggest a relative loss of ILC2s rather than a conversion, in accordance with a previous report (O'Sullivan et al., 2016).

To investigate the potential contribution of inflammatory cytokines to obesity-associated immune disorders, WT, tumor necrosis factor (TNF), and IFN-γ-deficient C57BL/6 mice were placed on a HFD. All WT mice were obese by weeks 10–12, weighing ~50%–100% more than WT mice fed a standard diet (Figure 1A). WT and IFN-γ-deficient mice displayed similar weight gain when submitted to an HFD (Figure S3), in contrast to TNF KO mice, which retained a leaner phenotype (Figure 1A). These observations indicate that TNF was implicated in adiposity, whereas IFN-γ was dispensable.

We next compared the functional features of ILC2s in the visceral adipose tissue of the same mice and found a correlation between weight gain and a decreased number of intracellular IL-5 and IL-13-expressing ILC2s in the HFD group in WT, but not in TNF KO, mice (Figure 1A). A similar decrease in IL-13-producing ILC2s was noted in obese WT and IFN-γ-KO mice (Figure S3). The proportion of M2-type macrophages expressing RELMα (Raes et al., 2002) followed the same trend (Figures 1B and S3). We conclude that TNF was involved in obesity-induced inflammation and ILC2-M2 dysregulation in obese mice.

We next sought to determine the factor(s) responsible for impaired ILC2 function. Extrinsic factors may include a defect in the production of epithelial alarmins (IL-25 and IL-33) (Saenz et al., 2013) and/or immune growth factors (such as IL-2 and IL-7) (Van Gool et al., 2014; Robinette et al., 2017), which sustain the number and function of ILC2s. Intrinsic factors may involve altered expression of activating and/or inhibitory receptors, such as ICOS, PD-1, and KLRG1 (Hoyler et al., 2012; Neill et al., 2010; Taylor et al., 2017). We compared the phenotype of ILC2s in WT and genetically deficient mice under standard or high-fat feeding. Dysfunctional ILC2s (i.e., in obese mice) expressed higher levels of the inhibitory receptor PD-1 than ILC2s from mice fed a standard diet; a 2- to 5-fold increase in the proportion of PD-1$^+$ cells among ILC2s and an increase in PD-1 expression (mean fluorescence intensity [MFI]) were noted in all experiments (Figure 1C). Of note, the data in Figure 1C indicate that the majority of IL-13$^+$ ILC2s expressed low levels of PD-1 in lean mice. The increase in PD-1 expression was noted only in mice gaining weight (i.e., WT and IFN-γ-KO mice) and not in TNF-deficient mice placed on a HFD, establishing a

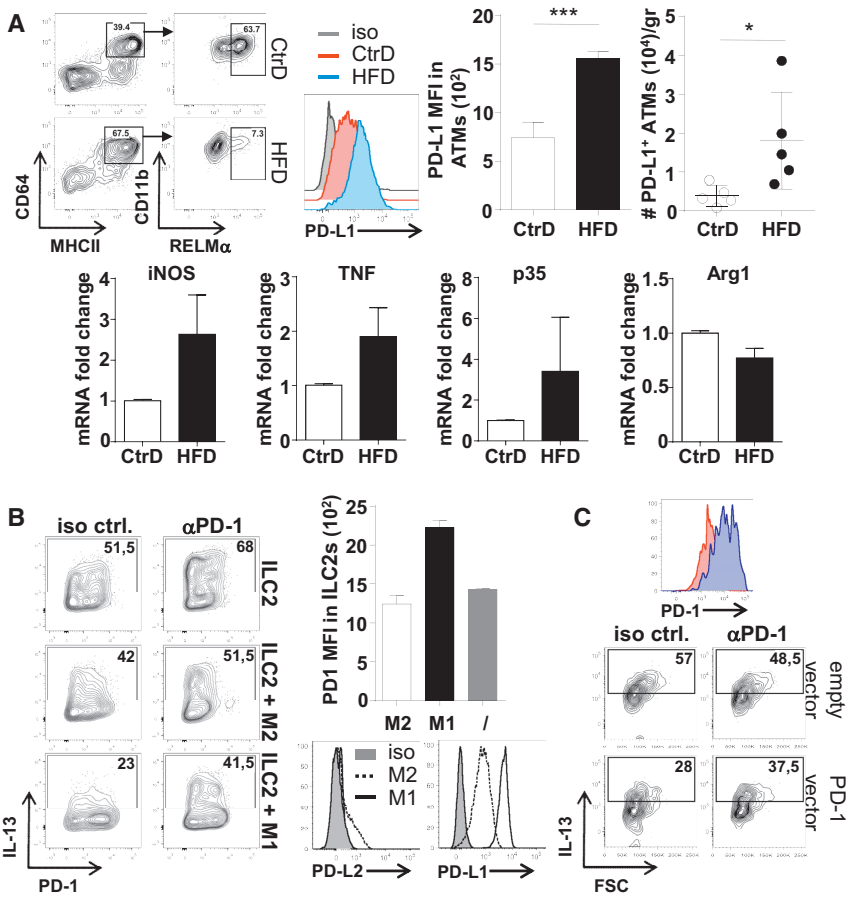

Figure 2. Increased Numbers of M1-type Macrophages Expressing PD-L1 in Obese Mice

(A) Gating strategy and proportion of RELMα$^+$ cells (left) and PD-L1 expression (intensity of expression and absolute numbers per gram of fat) (right) in ATMs from lean and obese WT mice. Error bars represent the SD of the mean (n = 5 mice). A non-parametric Mann-Whitney *U* test was used to determine statistical differences (*p < 0.05; ***p < 0.001). Expression of iNOS, TNF, p35, and Arg1 mRNA (3 biological replicates ± SD, bottom graphs) in ATMs sorted from 5 pooled lean and obese mice.

(B) Expression of IL-13 (frequency of IL-13$^+$ cells in quadrant of fluorescence-activated cell sorted [FACS] plots) and PD-1 in ILC2s sorted from the visceral adipose tissue of lean mice (10 pooled mice), expanded with IL-2-IL-7-IL-33, and cultured alone or with M2 or M1 bone-marrow-derived macrophages in the presence of IL-2-IL-7-IL-33 and anti-PD-1 or isotype control mAb and brefeldin after 48 hr. Bar graphs show the intensity of PD-1 expression in ILC2s (with technical duplicates), and histograms show PD-L1 and PD-L2 expression in M1 and M2 macrophages.

(C) Expression of PD-1 and IL-13 in ILC2s retrovirally transduced to overexpress GFP (empty vector, pink) or GFP and PD-1 (PD-1 vector, blue), sorted based on GFP expression, expanded for 3 days in IL-2, and cultured alone or with anti-PD-1 mAb in presence of IL-2-IL-7-IL-33 and brefeldin after 24 hr.

Data are representative of 3 (A and B) and 2 (C) independent experiments.

correlation between PD-1 expression, ILC2 dysfunction, and consequently impaired beige adipocyte function (Figures 1E and S3). By contrast, KLRG1 was expressed by all ILC2s in both lean and obese mice, and ICOS was slightly upregulated in a minor population of ILC2s, regardless of PD-1 expression (Figure 1D).

M1-type Macrophages Express PD-L1 and Inhibit ILC2 Function *In Vitro*

We next examined whether the expression of the PD-L1 was also regulated in the visceral adipose tissue during chronic inflammation. The data in Figure 2A show that MHCII$^+$ CD64$^+$ cells, which mainly represent macrophages (Tamoutounour et al., 2012), displayed increased levels of PD-L1 in WT obese mice. Of note, two major changes were noted in the adipose tissue of HFD-fed mice: the proportion of live macrophages increased by more than 50%, and their phenotype and function shifted from an M2-type to an M1-type characterized by decreased levels of intracellular RELMα, decreased expression of Arg1 mRNA, and increased expression of mRNA coding for iNOS, TNF, and IL-12p35 (Figure 2A). Thus, the proportion of M2-type cells decreased from 63% to 7% in HFD- versus standard-fed mice, with a concomitant 4-fold increase in the absolute number of PD-L1$^+$ macrophages (per gram of fat). These observations suggest that the PD-1-PD-L1 pathway may play a role in ILC2 dysregulation.

To get better insight into the role of macrophages, we co-cultured ILC2s (isolated from the adipose tissue of untreated mice and expanded *in vitro*) with M1 or M2-type macrophages differentiated *in vitro* from bone marrow cells. The data in Figure 2B show that ILC2s expressed increased surface levels of PD-1 and decreased intracellular IL-13 when co-cultured with M1 macrophages compared to cultures of ILC2s alone or with M2 cells. In addition, M1 macrophages expressed higher levels of PD-L1 than M2 macrophages (Figure 2B). Of note, PD-1 blockade strongly enhanced IL-13 expression in ILC2-M1 co-cultures. Addition of neutralizing anti-PD-1 monoclonal antibodies (mAbs) also enhanced IL-13 expression in cultures of ILC2s alone or ILC2-M2, an observation in line with a report showing that ILC2s may express PD-L1 in some conditions; i.e., in presence of IL-33 (Schwartz et al., 2017). Finally, overexpression of PD-1 in cultured ILC2s resulted in decreased IL-13 expression, which was partially restored by addition of neutralizing mAb (Figure 2C).

Injection of TNF Impairs ILC2 Function and Upregulates PD-1 Expression in an IL-33-Dependent Manner

The deleterious effect of TNF in obesity has been recognized for more than 25 years (Hotamisligil et al., 1993; Kern et al., 1995), but its mechanism of action remains elusive. To test whether this cytokine may affect ILC2s, we injected 1 μg TNF in naive

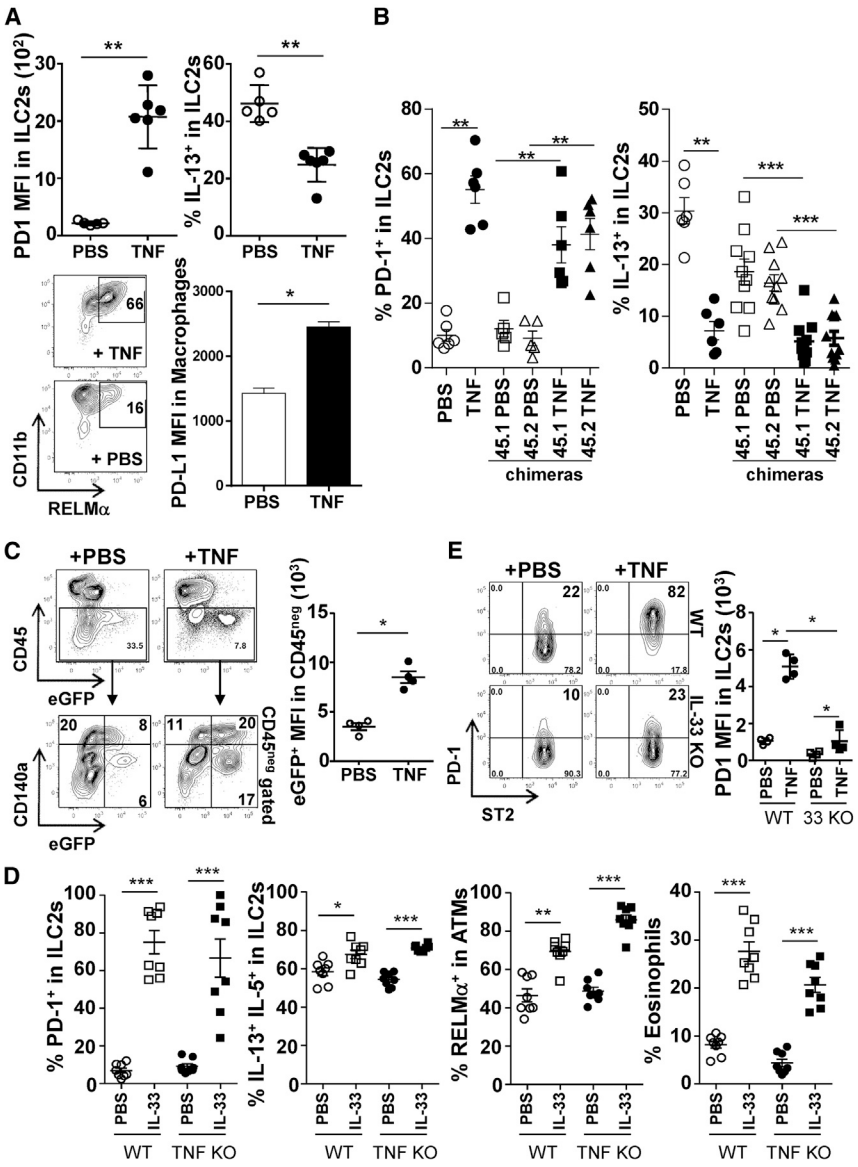

Figure 3. TNF Upregulates PD-1 Expression in ILC2s by Triggering IL-33

(A) Expression of PD-1 (MFI) and frequency of IL-13$^+$ cells (left graphs) in ILC2s from WT mice injected intraperitoneally (i.p.) with 1 μg recombinant TNF (rTNF; days 0 and 1) purified from adipose tissue at day 2 and restimulated shortly with PMA-ionomycin in the presence of brefeldin A. Also shown is the expression of RELMα and CD11b (FACS plots) and PD-L1 (MFI, bar graphs) in ATMs from the same mice.

(B) Frequency of PD1$^+$ and IL-13$^+$ cells in CD45.1$^+$ or CD45.2$^+$ ILC2s from WT or chimeric mice (CD90.1 C57BL/6 mice irradiated and reconstituted with a 50:50 mix of bone marrow from WT CD45.1 and TNFRI KO CD45.2 donors) and treated or not with rTNF.

(C) Gating strategy and expression of CD45 and CD140a, and EGFP in CD45$^-$ cells from the stromal vascular fraction of IL-33^{EGFP} mice treated or not with rTNF.

(D) Frequency of PD-1$^+$ and IL-13$^+$IL-5$^+$ cells in ILC2s, RELMα$^+$ in ATMs, and Siglec$^+$ eosinophils in the stromal fraction of the visceral adipose tissue of WT and TNF KO mice injected or not with recombinant IL-33 (rIL-33).

(E) Frequency of PD-1$^+$ cells (numbers in quadrant) and intensity of PD-1 expression in ST2$^+$ ILC2s from WT and IL-33 KO mice treated or not with rTNF.

Data are representative of 6 (A), 2 (B–D), and 3 (E) independent experiments. Error bars represent the SD of the mean (n = 5–10 mice per group). A non-parametric Mann-Whitney *U* test was used to determine statistical differences (*p < 0.05, **p < 0.01, and ***p < 0.001).

mice at days 0 and 1 and monitored the phenotype and function of ILC2s at day 2. The data in Figure 3A indicate that exogenous TNF recapitulated some features of obesity, namely the loss of functional ILC2s and the increase in PD-1 expression, and correlated with the development and recruitment of M1-type macrophages expressing high levels of PD-L1, at the expense of PD-L1^{int} M2-type cells. This loss was dependent on the expression of TNFR1 (Figure S4).

We next used WT and TNFR1 KO chimeras to test whether TNF acted on ILC2s directly or indirectly. Lethally irradiated WT C57BL/6 recipient mice were transplanted with WT and TNFR1 KO bone marrow at an equal ratio and injected 10 weeks later with 1 μg TNF. The function of ILC2s from either strain was impaired, as assessed by increased PD-1 expression and decreased IL-13 production (Figure 3B), indicating that the effect of TNF on ILC2s was indirect.

Among the factors induced by TNF, IL-33 is a likely candidate, as it is expressed by TNF-treated human pre-adipocytes (Wood et al., 2009) and was shown to upregulate PD-1 on murine ILC2s in response to IL-2 and IL-7 stimulation *in vitro* (Taylor et al., 2017). We therefore undertook a series of experiments to evaluate the role of IL-33 in TNF-induced ILC2 dysregulation *in vivo*. Using IL-33-reporter mice, we first showed that TNF injection led to an increased proportion of IL-33-competent cells and increased levels of EGFP expression among CD45^{neg} CD140a$^{hi/int}$ cells, defined as pre-adipocytes (Berry and Rodeheffer, 2013; Lee et al., 2012) (Figure 3C). Second, injection of IL-33 resulted in increased PD-1 expression on ILC2s in both WT and TNF KO mice (Figure 3D), indicating that it acts downstream of TNF. Third, injection of TNF increased PD-1 expression to a much lower extent in IL-33 KO mice than in WT mice (Figure 3E), suggesting that IL-33 was required for optimal TNF-induced PD-1 upregulation. Interestingly, the injection of IL-33 in WT mice increased the proportion and intensity of PD-1-expressing ILC2s but did not impair their function (Figure 3D). Their intact capacity to produce IL-5 and IL-13 was correlated with the maintenance of M2-type macrophages (Kurowska-Stolarska et al., 2009) (which expressed lower levels of

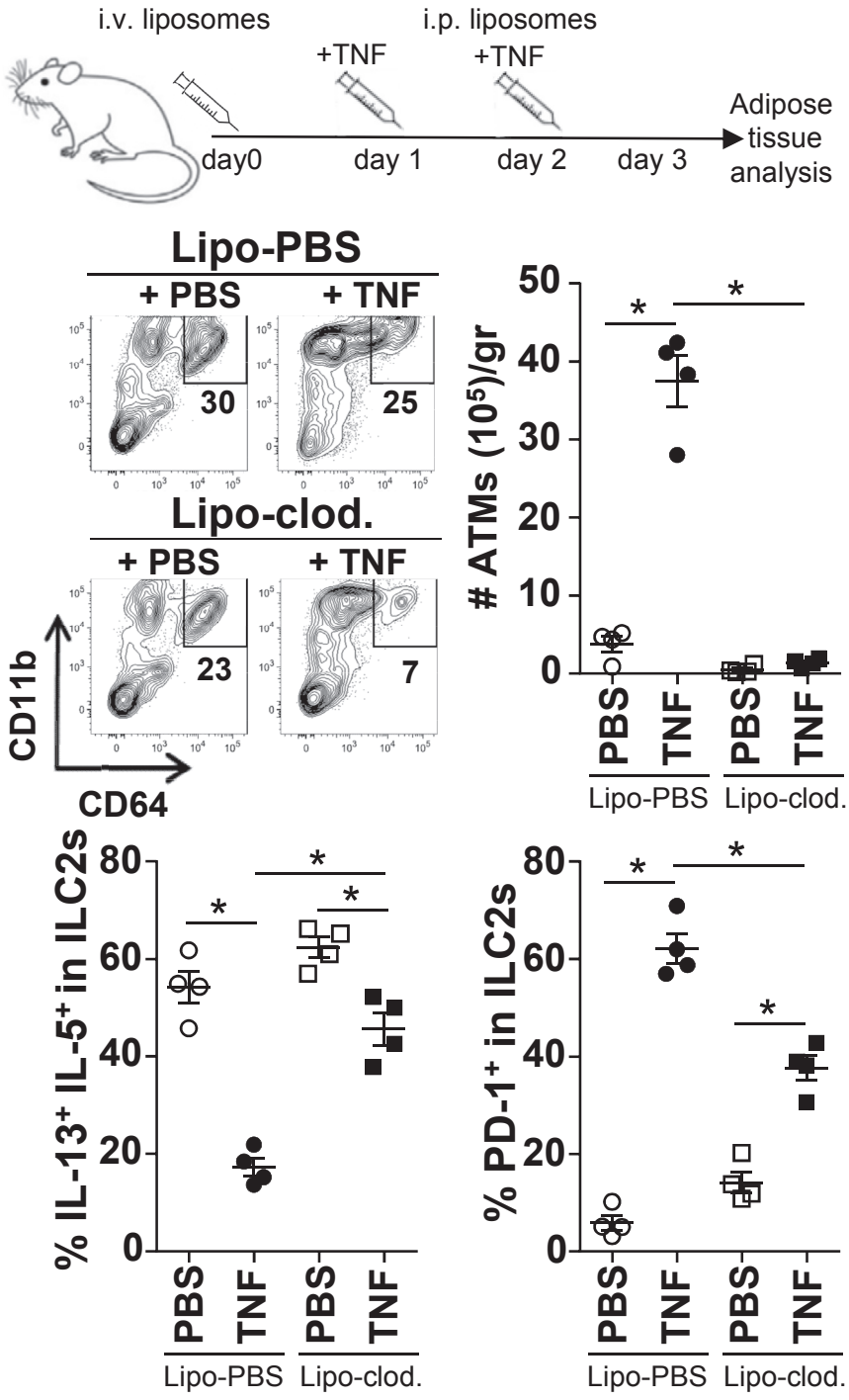

Figure 4. Depletion of Inflammatory Macrophages Rescues ILC2 Function in TNF-Treated Mice

Expression of CD11b and CD64, number of ATMs, and frequency of IL13$^+$ IL-5$^+$ (after a short restimulation with PMA-ionomycin in the presence of brefeldin A) and PD-1$^+$ cells in ILC2s from visceral adipose tissue from WT mice injected with PBS or clodronate liposomes and treated with PBS or rTNF. Error bars represent the SD of the mean of 4 individual mice (n = 4). A non-parametric Mann-Whitney *U* test was used to determine statistical differences (*p < 0.05). Each dot plot is representative of 1 mouse. Data are representative of 3 independent experiments.

PD-L1 than M1-type macrophages; see Figure 2), suggesting a role for PD-L1$^+$ M1 macrophages in TNF-induced loss of ILC2s.

Depletion of Inflammatory Macrophages Rescues ILC2 Function

To evaluate the role of inflammatory macrophages in ILC2 dysregulation *in vivo*, we injected clodronate liposomes in mice prior to TNF injection, a protocol that efficiently depleted visceral adipose tissue macrophages and/or prevented their recruitment (Van Rooijen and Sanders, 1994). The proportion of ILC2s producing IL-13 and IL-5 was only slightly decreased in these mice and remained 2.5-fold higher than in mice treated with control liposomes (Figure 4). Unexpectedly, PD-1 expression was significantly reduced in the absence of macrophages, suggesting that macrophages may favor not only PD-1 engagement through high PD-L1 expression but also increased PD-1 expression on ILC2s. Thus, TNF signaling regulated two steps in adipose tissue. First, it induced PD-1 upregulation on ILC2 indirectly via IL-33. Second, it activated the differentiation and recruitment of M1-type macrophages expressing higher levels of PD-L1 compared to M2 macrophages in steady state.

PD-1 Blockade Partially Restores the ILC2-Eosinophil-Alternatively Activated Macrophage Axis

Finally, we tested whether PD-1 blockade *in vivo* may ameliorate tissue homeostasis in obese mice. C57BL/6 male mice were placed on a HFD starting at 8 weeks of age and treated with 7 injections of 200 μg anti-PD-1 (or isotype control) mAb from weeks 11–13. The data in Figure 5A indicate that inhibition of PD-1 signaling significantly increased the proportion of ILC2s expressing IL-13 but did not restore the number of IL-13$^+$ ILC2s to control levels. However, the absolute number of eosinophils and alternatively activated macrophages was strongly increased, suggesting an improved function of ILC2s. In addition, anti-PD1 treatment restored the expression of IL-5 and IL-13 mRNA by the vascular stromal fraction to control levels (of standard-diet-fed mice) and

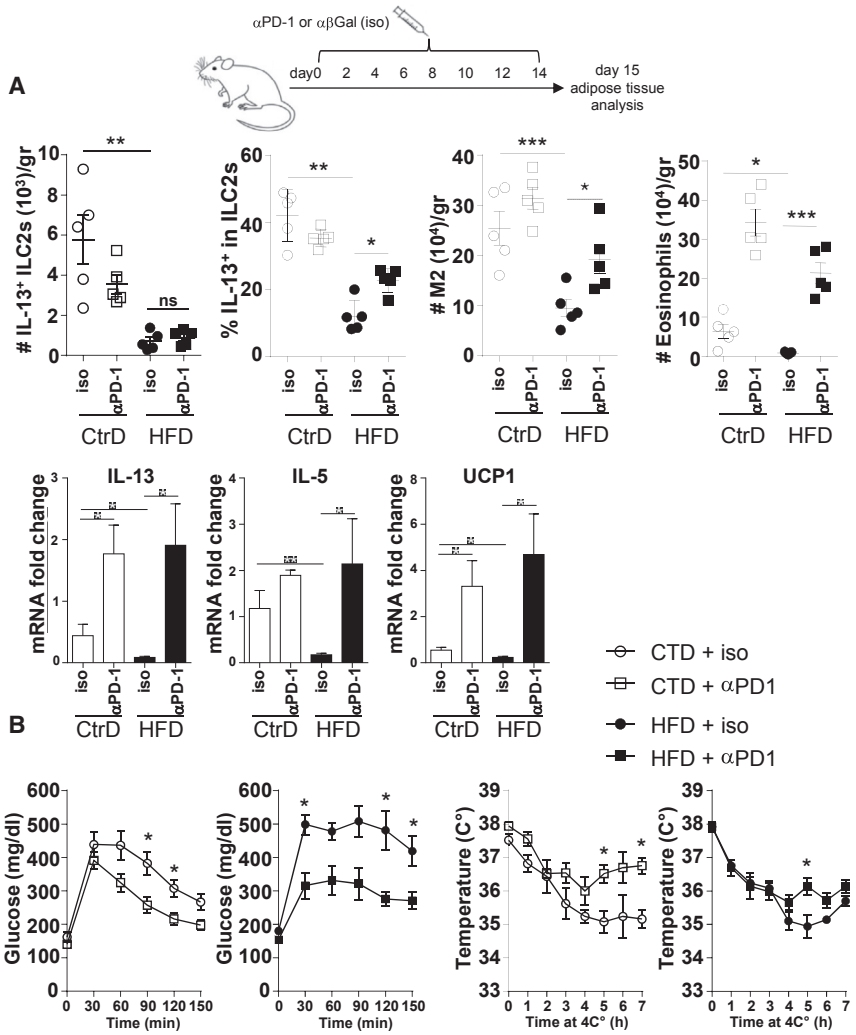

Figure 5. PD-1 Blockade Partially Restores the Type 2 Innate Response and Ameliorates Tissue Homeostasis

(A) Number of IL-13$^+$ ILC2s, M2 macrophages, and eosinophils per gram of fat and frequency of IL-13$^+$ cells in ILC2s (top graphs), and expression of IL-13, IL-5, and UCP1 mRNA (bottom graphs) in the stromal vascular fraction of mice fed with control or HFD and treated or not with anti-PD-1 mAb. For cytokine detection, cells were briefly stimulated with PMA-ionomycin in the presence of brefeldin A.

(B) Assessment of glucose tolerance (left graphs) and resistance to 7-hr cold exposure (4C°) (right graphs) in mice fasted overnight.

Data are representative of 3 (A) and 2 (B) independent experiments. Error bars represent the SD of the mean (n = 5 mice per group). A non-parametric Mann-Whitney *U* test was used to determine statistical differences (*p < 0.05; **p < 0.01; ***p < 0.001, ns, not significant).

enhanced the level of mRNA coding for uncoupling protein 1 (UCP1), which is involved in the process of beiging (Figure 5A). We next tested the effect of PD-1 blockade on whole-body metabolism and found that anti-PD1 treatment ameliorated glucose intolerance and the adaptation to environmental cold in lean and obese mice (Figure 5B). Collectively, these data suggest that PD-1 blockade partially restores the function of the type 2 innate axis, with a beneficial effect on adipose tissue homeostasis and beiging.

DISCUSSION

ILC2s appear as central regulators of adipose tissue homeostasis and are profoundly altered in obese humans and mice. The main objective of this work was to decipher the cellular and molecular mechanisms causing ILC2 dysfunction in obese mice. Our observations point to a major role of PD-1 as an intrinsic negative regulator of ILC2 function in high-fat-diet fed mice, as assessed by (1) the upregulation of PD-1 expression on ILC2 from obese mice; (2) the strict correlation between increased PD-1 expression, diminished IL-5 and IL-13 production, and weight gain; and (3) the amelioration of the ILC2-eosinophil-alternatively activated macrophage axis, glucose tolerance, and cold resistance following PD-1 blockade *in vivo*. These data, together with our results showing that anti-PD-1 antibodies restore ILC2 function *in vitro* (in the absence of other PD-1$^+$ cells), suggest that the PD-1 engagement on ILC2s strongly contributes to the loss of the "Th2 environment" in HFD mice.

Our data identify the alarmin IL-33 as the predominant factor upregulating PD-1 expression on ILC2s. Using a model that recapitulates some of the HFD-induced perturbations on ILC2s, we show that TNF triggered the expression of IL-33 by pre-adipocytes and promoted the differentiation of PD-L1$^+$ M1-type macrophages. Both steps were necessary for ILC2 dysregulation. Although IL-33 can be expressed by a variety of hematopoietic and nonhematopoietic cells (Balzola et al., 2010; Schmitz et al., 2005; Zeyda et al., 2013), the major source of the IL-33 protein in our setting was the CD45$^-$ CD140a$^+$ population, defined as pre-adipocytes (Lee et al., 2012).

Our observations are consistent with a report showing that the level of IL-33 mRNA in human adipocytes was increased by TNF *in vitro* (Wood et al., 2009). Expression of IL-33 and its receptor was also markedly elevated in the adipose tissue of obese humans, with endothelial cells representing the main source (Zeyda et al., 2013). By contrast, adipose expression and circulating IL-33 was shown to be downregulated in obese mice (Ding et al., 2016), an observation that was interpreted as the potential cause of the ILC2 loss. However, based on our data in TNF-injected mice (whose protein levels are increased upon TNF injection), we suggest that IL-33 may display opposite functions in ILC2s, maintaining their homeostasis and function in steady

state while triggering the expression and inhibitory function of PD-1 in inflammatory conditions in obese mice (i.e., in the presence of PD-L1-expressing cells).

Our observations highlight the major role of monocytes-macrophages in the dysregulation of the type 2 innate response. HFD feeding or injections of TNF resulted in the recruitment and/or differentiation of inflammatory monocytes. TNF can act in diverse ways, by (1) favoring the recruitment, survival, and function of M1-type macrophages in a cell-extrinsic and cell-intrinsic manner (Wolf et al., 2017b); (2) counteracting the emergence of M2 macrophages (Kratochvill et al., 2015); and (3) blocking IL-13 production by eosinophils (Kratochvill et al., 2015). Although the source of TNF in our setting remains to be established, data in the literature suggest that monocytes-macrophages and adipocytes are the major producers in obesity (Hotamisligil et al., 1993; De Taeye et al., 2007). In particular, Patsouris et al. (2008) reported that ablation of CD11c-positive cells (inflammatory macrophages) in obese mice reduced, but did not ablate, TNF levels and inflammatory responses in adipose tissue. The critical role of monocytes-macrophages in the deregulation of the type 2 immune response was suggested by our findings that macrophage ablation prevented ILC2 dysregulation by TNF *in vivo* and that M1-type macrophages inhibited ILC2 function *in vitro* in a PD-1 dependent manner. Accordingly, two reports demonstrate that macrophage ablation resulted in normalization of insulin sensitivity (Feng et al., 2011; Patsouris et al., 2008). It is likely that macrophages play a dual role: secreting TNF and expressing PD-L1, as TNF has been identified as a very potent signal for PD-L1 upregulation on monocytes *in vitro* and *in vivo* (Hartley et al., 2017).

In conclusion, the data presented herein clarify some aspects of the deleterious role of TNF in obesity reported 25 years ago (Hotamisligil et al., 1993). Our observations would be compatible with a scenario in which, upon high-fat feeding, adipocyte hypertrophy and necrosis would create an inflammatory environment through immunogenic cell death and/or secretion of adipokines and fatty acids (Shi et al., 2006; Sun et al., 2011). TNF seems to play a central role in the disruption of homeostasis by triggering the PD-1-PD-L1 pathway through IL-33 induction and activating M1-type macrophages. The engagement of PD-1 on ILC2s with PD-L1 expressed by macrophages would induce a negative signal in ILC2s and destabilize the entire type 2 innate axis (including eosinophils and type 2 macrophages) (this report).

It is likely that increased PD-1 signaling in ILC2s will affect several circuits of beiging in HFD-fed mice, thereby resulting in major impairment of weight control. Indeed, ILC2s not only are a direct source of methionine-enkephalin peptides that stimulate activity of beige adipose tissue but also sustain the number and function of eosinophils and alternatively activated macrophages, which through the secretion of IL-4 and norepinephrine, respectively, also activate beiging. Interfering with PD-1 signaling may therefore have a multiplying beneficial effect and restore tissue homeostasis in various immune disorders.

STAR★METHODS

Detailed methods are provided in the online version of this paper and include the following:

SUPPLEMENTAL INFORMATION

Supplemental Information includes four figures and one table and can be found with this article online at https://doi.org/10.1016/j.celrep.2018.10.091.

ACKNOWLEDGMENTS

We thank O. Leo for interesting discussions and C. Abdelaziz and V. Dissy for animal care.

This work was supported by the Belgian Program in Interuniversity Poles of Attraction initiated by the Belgian State, by grants from the Fonds Jean Brachet, the European Regional Development Fund (ERDF-Wallonia BioMed 2014-2020-LIV 45-20), Wallonia (Programme d'Excellence Food4Gut), and the National Fund for Scientific Research.

AUTHOR CONTRIBUTIONS

G.O., E.B., A.T., and M.M. designed the study and analyzed data; G.O., E.B., and A.T. performed most experiments, with contributions from L. Bonetti, V.A., and K.E.; B.R. and M.L.B. provided transgenic mice; L. Boon provided reagents; and G.O. and M.M. supervised the study and wrote the paper.

DECLARATION OF INTERESTS

The authors declare no competing interests.

Received: September 7, 2017
Revised: June 19, 2018
Accepted: October 24, 2018
Published: November 20, 2018

REFERENCES

Balzola, F., Bernstein, C., Ho, G.T., and Lees, C. (2010). Epithelial-derived IL-33 and its receptor ST2 are dysregulated in ulcerative colitis and in experimental TH1/TH2 driven enteritis. Inflamm. Bowel Dis. Monit. *11*, 30.

Berry, R., and Rodeheffer, M.S. (2013). Characterization of the adipocyte cellular lineage in vivo. Nat. Cell Biol. *15*, 302–308.

Brestoff, J.R., Kim, B.S., Saenz, S.A., Stine, R.R., Monticelli, L.A., Sonnenberg, G.F., Thome, J.J., Farber, D.L., Lutfy, K., Seale, P., and Artis, D. (2015). Group 2 innate lymphoid cells promote beiging of white adipose tissue and limit obesity. Nature *519*, 242–246.

De Taeye, B.M., Novitskaya, T., McGuinness, O.P., Gleaves, L., Medda, M., Covington, J.W., and Vaughan, D.E. (2007). Macrophage TNF-α contributes

to insulin resistance and hepatic steatosis in diet-induced obesity. Am. J. Physiol. Endocrinol. Metab. *293*, E713–E725.

Ding, X., Luo, Y., Zhang, X., Zheng, H., Yang, X., Yang, X., and Liu, M. (2016). IL-33-driven ILC2/eosinophil axis in fat is induced by sympathetic tone and suppressed by obesity. J. Endocrinol. *231*, 35–48.

Feng, B., Jiao, P., Nie, Y., Kim, T., Jun, D., van Rooijen, N., Yang, Z., and Xu, H. (2011). Clodronate liposomes improve metabolic profile and reduce visceral adipose macrophage content in diet-induced obese mice. PLoS ONE *6*, e24358.

Hartley, G., Regan, D., Guth, A., and Dow, S. (2017). Regulation of PD-L1 expression on murine tumor-associated monocytes and macrophages by locally produced TNF-α. Cancer Immunol. Immunother. *66*, 523–535.

Hotamisligil, G.S., Shargill, N.S., and Spiegelman, B.M. (1993). Adipose expression of tumor necrosis factor-alpha: direct role in obesity-linked insulin resistance. Science *259*, 87–91.

Hoyler, T., Klose, C.S.N., Souabni, A., Turqueti-Neves, A., Pfeifer, D., Rawlins, E.L., Voehringer, D., Busslinger, M., and Diefenbach, A. (2012). The transcription factor GATA-3 controls cell fate and maintenance of type 2 innate lymphoid cells. Immunity *37*, 634–648.

Kanneganti, T.-D., and Dixit, V.D. (2012). Immunological complications of obesity. Nat. Immunol. *13*, 707–712.

Kern, P.A., Saghizadeh, M., Ong, J.M., Bosch, R.J., Deem, R., and Simsolo, R.B. (1995). The expression of tumor necrosis factor in human adipose tissue. Regulation by obesity, weight loss, and relationship to lipoprotein lipase. J. Clin. Invest. *95*, 2111–2119.

Kitamura, T., Koshino, Y., Shibata, F., Oki, T., Nakajima, H., Nosaka, T., and Kumagai, H. (2003). Retrovirus-mediated gene transfer and expression cloning: powerful tools in functional genomics. Exp. Hematol. *31*, 1007–1014.

Kratochvill, F., Neale, G., Haverkamp, J.M., Van de Velde, L.A., Smith, A.M., Kawauchi, D., McEvoy, J., Roussel, M.F., Dyer, M.A., Qualls, J.E., and Murray, P.J. (2015). TNF counterbalances the emergence of M2 tumor macrophages. Cell Rep. *12*, 1902–1914.

Kurowska-Stolarska, M., Stolarski, B., Kewin, P., Murphy, G., Corrigan, C.J., Ying, S., Pitman, N., Mirchandani, A., Rana, B., van Rooijen, N., et al. (2009). IL-33 amplifies the polarization of alternatively activated macrophages that contribute to airway inflammation. J. Immunol. *183*, 6469–6477.

Lee, Y.H., Petkova, A.P., Mottillo, E.P., and Granneman, J.G. (2012). In vivo identification of bipotential adipocyte progenitors recruited by β3-adrenoceptor activation and high-fat feeding. Cell Metab. *15*, 480–491.

Lim, A.I., Menegatti, S., Bustamante, J., Le Bourhis, L., Allez, M., Rogge, L., Casanova, J.-L., Yssel, H., and Di Santo, J.P. (2016). IL-12 drives functional plasticity of human group 2 innate lymphoid cells. J. Exp. Med. *213*, 569–583.

Molofsky, A.B., Nussbaum, J.C., Liang, H., Dyken, S.J. Van, Cheng, L.E., Mohapatra, A., Chawla, A., and Locksley, R.M. (2013). Innate lymphoid type 2 cells sustain visceral adipose tissue eosinophils and alternatively activated macrophages. J. Exp. Med. *210*, 535–549.

Molofsky, A.B., Van Gool, F., Liang, H.E., Van Dyken, S.J., Nussbaum, J.C., Lee, J., Bluestone, J.A., and Locksley, R.M. (2015). Interleukin-33 and interferon-γ counter-regulate group 2 innate lymphoid cell activation during immune perturbation. Immunity *43*, 161–174.

Moro, K., Kabata, H., Tanabe, M., Koga, S., Takeno, N., Mochizuki, M., Fukunaga, K., Asano, K., Betsuyaku, T., and Koyasu, S. (2016). Interferon and IL-27 antagonize the function of group 2 innate lymphoid cells and type 2 innate immune responses. Nat. Immunol. *17*, 76–86.

Neill, D.R., Wong, S.H., Bellosi, A., Flynn, R.J., Daly, M., Langford, T.K., Bucks, C., Kane, C.M., Fallon, P.G., Pannell, R., et al. (2010). Nuocytes represent a new innate effector leukocyte that mediates type-2 immunity. Nature *464*, 1367–1370.

O'Sullivan, T.E., Rapp, M., Fan, X., Walzer, T., Dannenberg, A.J., Sun, J.C., Weizman, O.-E., Bhardwaj, P., and Adams, N.M. (2016). Adipose-resident group 1 innate lymphoid cells promote obesity-associated insulin resistance. Immunity *45*, 428–441.

O'Rourke, R.W., White, A.E., Metcalf, M.D., Winters, B.R., Diggs, B.S., Zhu, X., and Marks, D.L. (2012). Systemic inflammation and insulin sensitivity in obese IFN-γ knockout mice. Metabolism *61*, 1152–1161.

Oboki, K., Ohno, T., Kajiwara, N., Arae, K., Morita, H., Ishii, A., Nambu, A., Abe, T., Kiyonari, H., Matsumoto, K., et al. (2010). IL-33 is a crucial amplifier of innate rather than acquired immunity. Proc. Natl. Acad. Sci. USA *107*, 18581–18586.

Patsouris, D., Li, P.P., Thapar, D., Chapman, J., Olefsky, J.M., and Neels, J.G. (2008). Ablation of CD11c-positive cells normalizes insulin sensitivity in obese insulin resistant animals. Cell Metab. *8*, 301–309.

Qiu, Y., Nguyen, K.D., Odegaard, J.I., Cui, X., Tian, X., Locksley, R.M., Palmiter, R.D., and Chawla, A. (2014). Eosinophils and type 2 cytokine signaling in macrophages orchestrate development of functional beige fat. Cell *157*, 1292–1308.

Raes, G., De Baetselier, P., Noël, W., Beschin, A., Brombacher, F., and Hassanzadeh Gh, G. (2002). Differential expression of FIZZ1 and Ym1 in alternatively versus classically activated macrophages. J. Leukoc. Biol. *71*, 597–602.

Robinette, M.L., Bando, J.K., Song, W., Ulland, T.K., Gilfillan, S., and Colonna, M. (2017). IL-15 sustains IL-7R-independent ILC2 and ILC3 development. Nat. Commun. *8*, 14601.

Saenz, S.A., Siracusa, M.C., Monticelli, L.A., Ziegler, C.G.K., Kim, B.S., Brestoff, J.R., Peterson, L.W., Wherry, E.J., Goldrath, A.W., Bhandoola, A., and Artis, D. (2013). IL-25 simultaneously elicits distinct populations of innate lymphoid cells and multipotent progenitor type 2 (MPPtype2) cells. J. Exp. Med. *210*, 1823–1837.

Schmitz, J., Owyang, A., Oldham, E., Song, Y., Murphy, E., McClanahan, T.K., Zurawski, G., Moshrefi, M., Qin, J., Li, X., et al. (2005). IL-33, an interleukin-1-like cytokine that signals via the IL-1 receptor-related protein ST2 and induces T helper type 2-associated cytokines. Immunity *23*, 479–490.

Schwartz, C., Khan, A.R., Floudas, A., Saunders, S.P., Hams, E., Rodewald, H.-R., McKenzie, A.N.J., and Fallon, P.G. (2017). ILC2s regulate adaptive Th2 cell functions via PD-L1 checkpoint control. J. Exp. Med. *214*, 2507–2521.

Shi, H., Kokoeva, M.V., Inouye, K., Tzameli, I., Yin, H., and Flier, J.S. (2006). TLR4 links innate immunity and fatty acid-induced insulin resistance. J. Clin. Invest. *116*, 3015–3025.

Sun, K., Kusminski, C.M., and Scherer, P.E. (2011). Adipose tissue remodeling and obesity. J. Clin. Invest. *121*, 2094–2101.

Tamoutounour, S., Henri, S., Lelouard, H., de Bovis, B., de Haar, C., van der Woude, C.J., Woltman, A.M., Reyal, Y., Bonnet, D., Sichien, D., et al. (2012). CD64 distinguishes macrophages from dendritic cells in the gut and reveals the Th1-inducing role of mesenteric lymph node macrophages during colitis. Eur. J. Immunol. *42*, 3150–3166.

Taylor, S., Huang, Y., Mallett, G., Stathopoulou, C., Felizardo, T.C., Sun, M.-A., Martin, E.L., Zhu, N., Woodward, E.L., Elias, M.S., et al. (2017). PD-1 regulates KLRG1 $^{+}$ group 2 innate lymphoid cells. J. Exp. Med. *214*, 1663–1678.

Van Gool, F., Molofsky, A.B., Morar, M.M., Rosenzwajg, M., Liang, H.E., Klatzmann, D., Locksley, R.M., and Bluestone, J.A. (2014). Interleukin-5-producing group 2 innate lymphoid cells control eosinophilia induced by interleukin-2 therapy. Blood *124*, 3572–3576.

Van Rooijen, N., and Sanders, A. (1994). Liposome mediated depletion of macrophages: mechanism of action, preparation of liposomes and applications. J. Immunol. Methods *174*, 83–93.

Wolf, Y., Boura-halfon, S., Cortese, N., Haimon, Z., Shalom, H.S., Kuperman, Y., Kalchenko, V., Brandis, A., David, E., Segal-hayoun, Y., et al. (2017a). Brown-adipose-tissue macrophages control tissue innervation and homeostatic energy expenditure. Nat. Immunol *18*, 665–674.

Wolf, Y., Shemer, A., Polonsky, M., Gross, M., Mildner, A., Yona, S., David, E., Kim, K.-W., Goldmann, T., Amit, I., et al. (2017b). Autonomous TNF is critical for in vivo monocyte survival in steady state and inflammation. J. Exp. Med. *214*, 905–917.

Wood, I.S., Wang, B., and Trayhurn, P. (2009). IL-33, a recently identified interleukin-1 gene family member, is expressed in human adipocytes. Biochem. Biophys. Res. Commun. *384*, 105–109.

Zeyda, M., Wernly, B., Demyanets, S., Kaun, C., Hämmerle, M., Hantusch, B., Schranz, M., Neuhofer, A., Itariu, B.K., Keck, M., et al. (2013). Severe obesity increases adipose tissue expression of interleukin-33 and its receptor ST2, both predominantly detectable in endothelial cells of human adipose tissue. Int. J. Obes. *37*, 658–665.

STAR★METHODS

KEY RESOURCES TABLE

REAGENT or RESOURCE	SOURCE	IDENTIFIER
Antibodies		
PE-Cy7 anti-CD90.2 (clone 53-2.1)	BD Biosciences	Cat#: 561642, RRID: AB_10895975
PE anti-IL33R(ST2) (clone U29-93)	BD Biosciences	Cat#: 566311, RRID: AB_2744490
PerCP eFluor 710 anti-ST2 (clone RMST2-33)	eBiosciences	Cat#: 46-9333-80, RRID: AB_2573880
BB515 anti-CD25 (clone PC61)	BD Biosciences	Cat#: 564424, RRID: AB_2738803
APC anti-CD127 (clone A7R34)	BD Biosciences	Cat#: 564175, RRID: AB_2732843
APC anti-CD279 (clone J43)	BD Biosciences	Cat#: 562671, RRID: AB_2737712
FITC anti-CD279 (clone J43)	eBiosciiences	Cat# 11-9985-81, RRID: AB_465471
AF700 anti-Ly-6A/E(Sca1) (clone D7)	eBiosciences	Cat#: 56-5981-82, RRID: AB_657836
PerCP eFluor 710 anti-KLRG1 (clone 2F1)	eBiosciences	Cat#: 46-5893-82, RRID: AB_10670282
BB515 anti-ICOS (clone C398.4A)	BD Biosciences	Cat#: 565881, RRID: AB_2744480
PE-cy7 anti-T-Bet (clone eBio4B10)	eBiosciences	Cat#: 25-5825-82, RRID: AB_11042699
A647 anti-RORγT (clone Q31-378)	BD Biosciences	Cat#: 562682, RRID: AB_2687546
PE anti-GATA3 (clone L50-823)	BD Biosciences	Cat#: 560074, RRID: AB_1645330
Biotin anti-CD49b (clone DX5)	BD Biosciences	Cat#: 553856, RRID: AB_395092
Biotin anti-CD3ε (clone 145-2C11)	eBiosciences	Cat#: 13-0031-82, RRID: AB_466319
Biotin ant-TCRγδ (clone eBioGL3)	BD Biosciences	Cat#: 553176, RRID: AB_394687
Biotin anti-Ter119 (clone TER119)	eBiosciences	Cat#: 13-5921-85, RRID: AB_466798
Biotin anti-CD19 (clone MB19-1)	eBiosciences	Cat#: 13-0191-85, RRID: AB_466385
Biotin anti-CD11c (clone N418)	eBiosciences	Cat#: 13-0114-82, RRID: AB_466363
PerCP-Cy5.5 anti-CD11c (clone N418)	BD Biosciences	Cat#: 560584, RRID: AB_1727422
Biotin anti-CD11b (clone M1/70)	eBiosciences	Cat#: 13-0112-85, RRID: AB_466360
AF700 anti-CD11b (clone M1/70)	BD Biosciences	Cat#: 557960, RRID: AB_396960
Biotin anti-CD4 (clone GK1.5)	eBiosciences	Cat#: 13-0041-82, RRID: AB_466325
Biotin anti-CD8α (clone 53-6.7)	eBiosicences	Cat#: 13-0081-85, RRID: AB_466347
Biotin anti-GR1 (clone RB6-8C5)	BD Biosciences	Cat#: 553124, RRID: AB_394640
PerCP-Cy5.5 Streptavidin	eBiosciences	Cat#: 45-4317-82, RRID: AB_10311495
Biotin anti-MHCII (clone M5/114.15.2)	eBiosciences	Cat#: 13-5321-85, RRID: AB_466663
PE-Cy7 strepatavidin	BD Biosciences	Cat#: 557598, RRID: AB_10049577
AF647 anti-CD64 (clone X54-5/7.1)	BD Biosciences	Cat#: 558539, RRID: AB_647120
PE anti-SiglecF (clone E50-2440)	BD Biosicences	Cat#: 552126, RRID: AB_394341
PE anti-CD273 (clone TY25)	BD Biosciences	Cat#: 557796, RRID: AB_396874
APC anti-CD273 (clone TY25)	BD Biosciences	Cat#: 560086, RRID: AB_1645223
APC anti-CD274 (clone MIH5)	BD Biosciences	Cat#: 564715, RRID: AB_2687479
PE-Cy7 anti-CD29 (clone eBio HMb1-1)	eBiosciences	Cat#: 25-0291-80, RRID: AB_1234964
APC anti-CD140a (clone D7)	eBiosciences	Cat#: 17-1401-81, RRID: AB_529482
PerCP-Cy5.5 anti-CD45 (clone 30-F11)	BD Biosciences	Cat#: 561869, RRID: AB_10895563
Rabbit anti-RELMα	PeproTech	Cat#: 500-P214, RRID: AB_1268332
FITC goat anti-rabbit Ig	BD Biosciences	Cat#: 554020, RRID: AB_395212
PE anti-IL13 (clone ebio13A)	eBiosciences	Cat#: 12-7133-81, RRID: AB_763561
APC anti-IL5 (clone TRFK5)	BD Biosciences	Cat#: 554396, RRID: AB_398548
Biotin anti-CD16/32 (clone 2.4G2)	BD Biosciences	Cat#: 553143, RRID: AB_394658
Anti-PD1 mAb (clone RMP1-14)	Bioceros	N/A
Anti-β Gal (clone GL117)	Bioceros	N/A

(*Continued on next page*)

Continued

REAGENT or RESOURCE	SOURCE	IDENTIFIER
Bacterial and Virus Strains		
NEB 5-alpha Competent *E. coli*	Biolabs	C2987I
Chemicals, Peptides, and Recombinant Proteins		
Recombinant mouse TNFα	Peprotech	Cat#: 315-01A
Recombinant mouse IL-33	Peprotech	Cat#: 210-33
Recombinant mouse IL-7	Peprotech	Cat#: 217-17
Recombinant mouse IL-2	Peprotech	Cat#: 212-12
D-glucose	Sigma Aldrich	Cat#: G7528
Live/dead stain	Invitrogen	Cat#: L34976
Clodronate	Liposoma B.V, the Netherlands	Cat#: CP-005
PMA	Sigma Aldritch	Cat#: P8139
Ionomycin	Sigma Aldritch	Cat#: I0634
Brefeldin A	Invitrogenn	Cat#: 00-4506-51
Collagenase, type 3	Worthington Biochemical corporation	Cat#: LS004183
Maxima SYBR Green/ROX qPCR Master Mix	Westburg	Cat#: TH K0223
Polybrène	Sigma Aldritch	Cat#: 107689
Ampicillin	Sigma Aldritch	Cat#: A9518
Puromycin	InvivoGen	Cat#: ant-pr
Critical Commercial Assays		
GenElute HP Endotoxin-Free Plasmid Maxiprep Kit	Sigma Aldritch	Cat#: NA0410
eBioscience Fixation/Perm diluent	Invitrogen	Cat#: 00-5223-56
eBioscience Fixation/Permeabilization concentrate	Invitrogen	Cat#: 00-5213-43
Permeabilization Buffer 10x	Invitrogen	Cat#: 00-8333-56
BD Perm/Wash	BD Biosciences	Cat#: 51-2091KZ
BD CytoFix/cytoperm	BD Biosciences	Cat#: 51-2090KZ
Deposited Data		
Experimental Models: Cell Lines		
Platinum-E (PlatE) retroviral packaging cell line	(Kitamura et al., 2003)	N/A
Experimental Models: Organisms/Strains		
Mouse: $Tnf^{tm1Gkl/J}$ Jax	The Jackson Laboratory	Stock#: 005540
Mouse: $Ifng^{tm1Ts/J}$ Jax	The Jackson Laboratory	Stock#: 002287
Mouse: $Tnfrsf1a^{tm1Imx}$ Jax	The Jackson Laboratory	Stock#: 003242
Mouse: IL-33KO	Oboki et al., 2010	N/A
Mouse: $IL\text{-}33^{eGFP}$	Oboki et al., 2010	N/A
Mouse: B6.SJL-*Ptprc*$^{a\ b}$/BoyJ	The Jackson Laboratory	Stock#: 002014
Mouse: B6.PL-*Thy1*^{a}/CyJ	The Jackson Laboratory	Stock#: 000406
Mouse: C57BL/6JOlaHsd	Envigo	Stock#: 5704F
Oligonucleotides		
See Table S1 for gene expression analysis primers	This paper	N/A
$Pdcd1^{Xho1\text{-}EcoR1}$-F: AATTAGATCTCTCGA GCCACCATGT GGGTCCGGCAGGTACC	This paper	N/A
$Pdcd1^{Xho1\text{-}EcoR1}$-R: GGGGGGGGCGGA ATTAAAGAGGC CAAGAACAATGTCC	This Paper	N/A
pMIEG (MCS)-F: CTACATCGTGACCTGGGAAG	This paper	N/A
pMIEG (MCS)-R: AAGGGTCGCTACAGACGTTG	This Paper	N/A
Recombinant DNA		
pMIEG-IRES-eGFP (retroviral transduction)	This paper	N/A
pMIEG-IRES-eGFP:Pdcd1 (retroviral transduction)	This paper	N/A

(*Continued on next page*)

Continued

REAGENT or RESOURCE	SOURCE	IDENTIFIER
Software and Algorithms		
FlowJo software version 9.6.4	Tree Star	N/A
GraphPad Prism 6	GraphPad software	N/A
Other		
Diet: High Fat Diet (HFD)	Research Diets, New Brunswick, NJ	D12492
Diet: Control Diet (CtrD)	Research Diets, New Brunswick, NJ	D12450B
StepOne Plus system	Applied Biosystems	N/A
BD FACS Aria III	BD Biosciences	N/A
BD Canto II	BD Biosciences	N/A

CONTACT FOR REAGENT AND RESOURCE SHARING

Further information and requests for resources and reagents should be directed and will be fulfilled by the Lead Contact, Guillaume Oldenhove (guillaume.oldenhove@ulb.ac.be).

EXPERIMENTAL MODEL AND SUBJECT DETAILS

Mice

C57BL/6 mice were purchased from Envigo. TNF KO ($Tnf^{tm1Gkl/J}$ Jax stock 005540), IFN-γ KO ($Ifng^{tm1Ts/J}$ Jax stock 002287), TNFRI KO ($Tnfrsf1a^{tm1Imx}$ Jax stock 003242), B6.SJL-Ptprca b/BoyJ and B6.PL-Thy1a/CyJ mice were purchased from The Jackson Laboratory. IL-33 KO were obtained by Susumu Nakae and the eGFP was revealed after deletion of the neo cassette (Oboki et al., 2010). Mice were maintained in a temperature-controlled (23 °C), specific pathogen-free facility with a strict 12 h light/dark cycle with free access to food and water and used at 8 to 10 weeks old at the beginning of the experiments. The experiments were carried out in accordance with the relevant European laws and institutional guidelines. We received specific approval for this study from the Animal Care and Use Committee of the Institute for Molecular Biology and Medicine (IBMM, ULB; protocol number CEBEA84).

METHOD DETAILS

Diet-induced obesity

Males were rendered obese upon feeding with the high fat diet (HFD) which contains 60% kcal fat, 20% kcal proteins and 20% kcal carbohydrate, starting at 8-weeks of age for 12-to-16 weeks. Control diet (CtrD) contains 10% kcal fat, 20% kcal proteins and 70% kcal carbohydrates. Body weight was measured weekly.

In vivo treatment

Mice were injected i.p. (d 0 and d 1) with 1 μg carrier-free rMuTNF or rMuIL-33 or with PBS alone. The adipose tissue was extracted at d 2. Some mice were injected i.p. with 200 μg of neutralizing anti-PD-1 mAb or isotype control anti-β Gal every other day for 2 weeks.

For glucose tolerance tests, mice were fasted overnight and injected i.p. with 2 g/kg D-glucose. Blood glucose values were measured just prior to injection (time 0) and at 30, 60, 90, 120 and 150 min post-injection. For the 4°C cold challenge, mice were shifted from 24 °C to 4 °C and body temperature was monitored every hour during 7 h

Generation of mixed BM chimeras

Bone marrow chimeric mice were generated by lethally irradiating CD90.1 mice with 650 Rads from a ^{137}Cs source delivered in two equal doses 4–5 h apart. After irradiation, mice were injected i.v. with a 50:50 mix of $8*10^6$ total bone marrow cells from WT CD90.2 CD45.1 and TNFR1 KO CD90.2 CD45.2 cells. 10 weeks later, mice were treated i.p. with rMuTNF or PBS.

Depletion of macrophages by administration of clodronate liposomes

Mice were injected i.v. or i.p. with 1 mg clodronate- or PBS-loaded liposomes at d 0 and 2, respectively, and further injected i.p. with 1 μg of TNF or PBS at d 1 and 2. The stromal vascular fraction was analyzed by flow cytometry at d 3.

Real-time quantitative PCR (qRT-PCR)

Total cellular RNA was extracted from cell lysates by the use of TRIzol reagent, and reverse transcription of mRNA was carried out using Superscript II reverse transcriptase (Invitrogen) according to the manufacturer's instructions. Quantitative PCR was performed

using a StepOne Plus system (Applied Biosystems, Foster City, CA) with Maxima SYBR Green/ROX qPCR Master Mix (Thermo Fisher Scientific, Waltham, MA). Quantification with RPL32 as endogenous housekeeping gene was done using standard curves.

Isolation of immune cells and flow cytometry

Perigonadal adipose tissue was used as representative visceral adipose tissue in all experiments. Adipose tissue was harvested and digested with 400 U/ml of collagenase type II at 37°C with shaking at 200 rpm for 30 min. Digested tissues were filtered through a 70 μm nylon mesh and centrifuged at 1600 rpm for 10 min. Floating adipocytes were removed, and the stromal vascular fraction (SVF) pellet was resuspended in red blood cell lysis buffer. Recovered cells were washed and stained with live/dead stain followed by standard surface staining with fluorochrome-conjugated antibodies listed in the Key Resources Table. ILC2s were identified as lineage negative (TCRγδ$^-$, DX5$^-$, CD3$^-$, CD4$^-$, CD8α$^-$, CD19$^-$, GR1$^-$, CD11b$^-$, CD11c$^-$), FSC/SSC-low-to moderate, CD90.2$^+$, CD127$^+$, CD25$^+$, Sca-1$^+$ and T1/ST2$^+$. Macrophages were identified as MHCII$^+$, CD11b$^+$, CD64$^+$ and eosinophils as SSC^{high}, MHCII$^-$, CD11b^{low}, SiglecF$^+$. Stromal cells and pre-adipocytes were identified as CD45$^-$, CD140a$^+$, CD29$^+$ and Sca-1$^+$. Single live cells were gated and cells were analyzed on a BD FACSCanto II and/or sorted using a BD FACSAria III. ILC2s were sorted as lineage negative, FSC/SSC-low-to moderate, CD90.2$^+$, Sca-1$^+$ and T1/ST2$^+$. Data were analyzed using FlowJo software version 9.6.4 (Tree Star, Inc.).

Intracellular cytokine detection

For intracellular staining of RELMα, cells were fixed and permeabilized with the Foxp3 staining set according to the manufacturer's protocol and were stained for 30 min at 4°C with rabbit anti-RELMα followed by incubation with goat anti-rabbit Ig-FITC for 30 min in the same buffer. For basal cytokine detection, single-cell suspensions were cultured in triplicate in a 96-well U-bottom plate in complete medium and stimulated for 3 h with 50 ng/ml PMA and 1 μg/ml ionomycin in the presence of brefeldin A. In the case of ILC2 cultures, cells were incubated only with brefeldin A. After 3 h, samples were stained for dead cells as described previously and then fixed and permeabilized. Intracellular staining was performed according to the BD Cytofix/Cytoperm kit protocol. ILC2s (identified as lineage negative, FSC/SSC-low-to moderate, CD90.2$^+$, Sca-1$^+$ and T1/ST2$^+$) were stained with anti-mouse IL-13 and anti-mouse/anti-human IL-5 or isotype controls: rat IgG1 (eBRG1) in the presence of anti-FcgIII/II receptor.

ILC2 culture

The stromal vascular fraction was extracted from perigonadal adipose tissue of 8 weeks old males. Cells were stained for CD90.2, Sca-1, CD127, CD25, T1/ST2 and for lineage markers (as described above) and ILC2s were purified by cell sorting. Sorted ILC2s were cultured in complete medium in the presence of IL-2, IL-7, and IL-33 (all at 50 ng/ml) for 7 to 10 d (fresh medium and cytokines were added every 2 d and the cultures were split into multiple wells). ILC2s were co-cultured during 48 h with bone marrow-derived macrophages (M1 or M2) in the presence of IL-2, IL-7, IL-33 (all at 10 ng/ml) with neutralizing anti-PD-1 or anti-β Gal mAbs as isotype control.

Retroviral transduction

The coding sequence of *Pdcd1* was cloned into the pMIEG-IRES-eGFP retroviral vector. All primers used for cloning *Pdcd1* are listed in the Key Resources Table. ILC2s were cell sorted from the visceral adipose tissue of mice fed with standard diet and expanded by rMuIL-2-IL-7-IL33 (all at 50 ng/ml). At day 3, cells were resuspended in retrovirus-containing supernatants plus 14 mg/ml of polybrene, followed by centrifugation (6000 g) for 90 min at 25 C°. Viral supernatant was removed and cells cultured for 3 days with rMuIL-2-IL-7-IL33, sorted based on GFP expression and expanded for 3 days in rMuIL-2 (10ng/ml). ILC2s were further cultured alone or with anti-PD-1 blocking antibody in presence of IL-2-IL-7-IL33 (all at 10 ng/ml) for 24 hours and analyzed for PD-1 and IL-13 expression following incubation in the presence of brefeldin A.

QANTIFICATION AND STATISTICAL ANALYSIS

Statistical analysis

Statistical analyses were performed using Prism6 (GraphPad Software, La Jolla, CA). Statistical significance was determined with the Mann–Whitney U-test for two-tailed data. Flow cytometry plots from Figures 1, 2A, 3 and 4 show one individual mouse representative of 4 to 5 mice. In Figure 2, they experiment was performed using cells pooled from 5 to 10 mice; number of biological replicates is indicated. Other data are shown as median ± standard error of the mean (SD). In Figures 1, 2A, 3, 4, and 5, ''n'' indicates the number of mice per group. For each figure, the number of experiments performed is indicated. A $p \leq 0.05$ value was considered significant and is denoted in figures as follows: *, $p < 0.05$; **, $p < 0.01$; ***, $p < 0.001$. No statistical methods were used to predetermine sample size. No animal or sample was excluded from the analysis.

Cell Reports, Volume *25*

Supplemental Information

PD-1 Is Involved in the Dysregulation of Type 2 Innate Lymphoid Cells in a Murine Model of Obesity

Guillaume Oldenhove, Elodie Boucquey, Anaelle Taquin, Valérie Acolty, Lynn Bonetti, Bernhard Ryffel, Marc Le Bert, Kevin Englebert, Louis Boon, and Muriel Moser

Supplemental Figure 1:

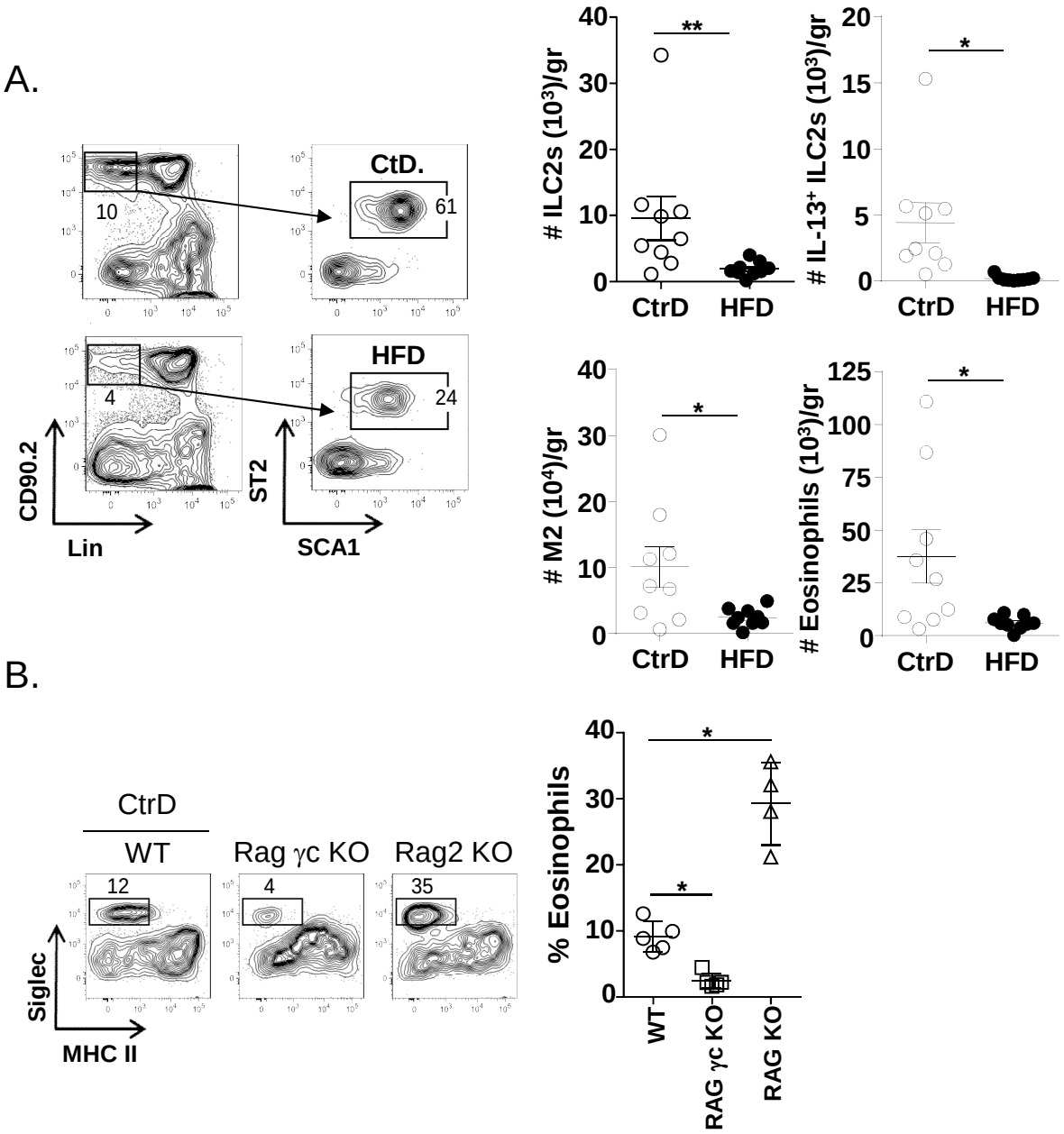

Supplemental Figure 1: Decrease in ILC2 number and functionality during obesity; related to figure 1. (**A**) The stromal vascular fraction from the visceral adipose tissue of WT C57BL/6 mice fed CtrD vs HFD for 12 weeks was analyzed by flow cytometry. Cells were briefly restimulated with PMA-ionomycin in the presence of brefeldin A and the absolute numbers of IL-13^{+} ILC2s (ILC2s identified as CD90.2^{+} lin^{-} Sca1^{+} ST2^{+} cells as illustrated by FACS plots, upper left panels), type 2 macrophages (defined as MHCII^{+} CD64^{+} CD11b^{+} RELMα^{+}) and eosinophils (defined as SSC^{high} MHCII^{-} CD11b^{low} Siglec^{+}) were determined per gram of fat. (**B**) The stromal vascular fraction from the visceral adipose tissue of WT C57BL/6, RAG γc KO and RAG KO mice fed standard diet was extracted and the percentage of eosinophils was analyzed by flow cytometry. Error bars represent the SDs of the means of 4-9 individual mice (*p <0.05). Data are representative of 4 (panel A) or 2 (Panel B) independent experiments.

Supplemental Figure 2:

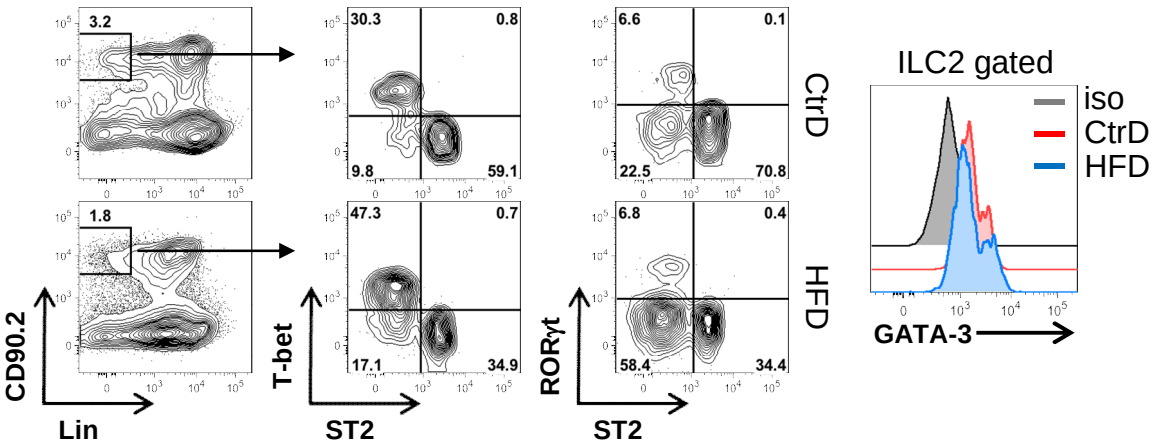

Supplemental Figure 2: **ILC2s maintain phenotypic stability during diet-induced obesity; related to figure 1.** 8 wk old males C57BL/6 WT were fed HFD or CtrD for 12 weeks and the stromal vascular fraction was extracted from the visceral adipose tissue. ILCs (defined as CD90.2^{+} lin^{-}) were analyzed by flow cytometry for their expression of ST2, T-bet, RORγt and GATA-3. FACS plots illustrate the gating strategy and the proportion of ILC2s expressing T-bet or RORγt. The histogram shows the expression of GATA3 by ILC2s. Data are representative of 2 independent experiments with similar results, n =5.

Supplemental Figure 3:

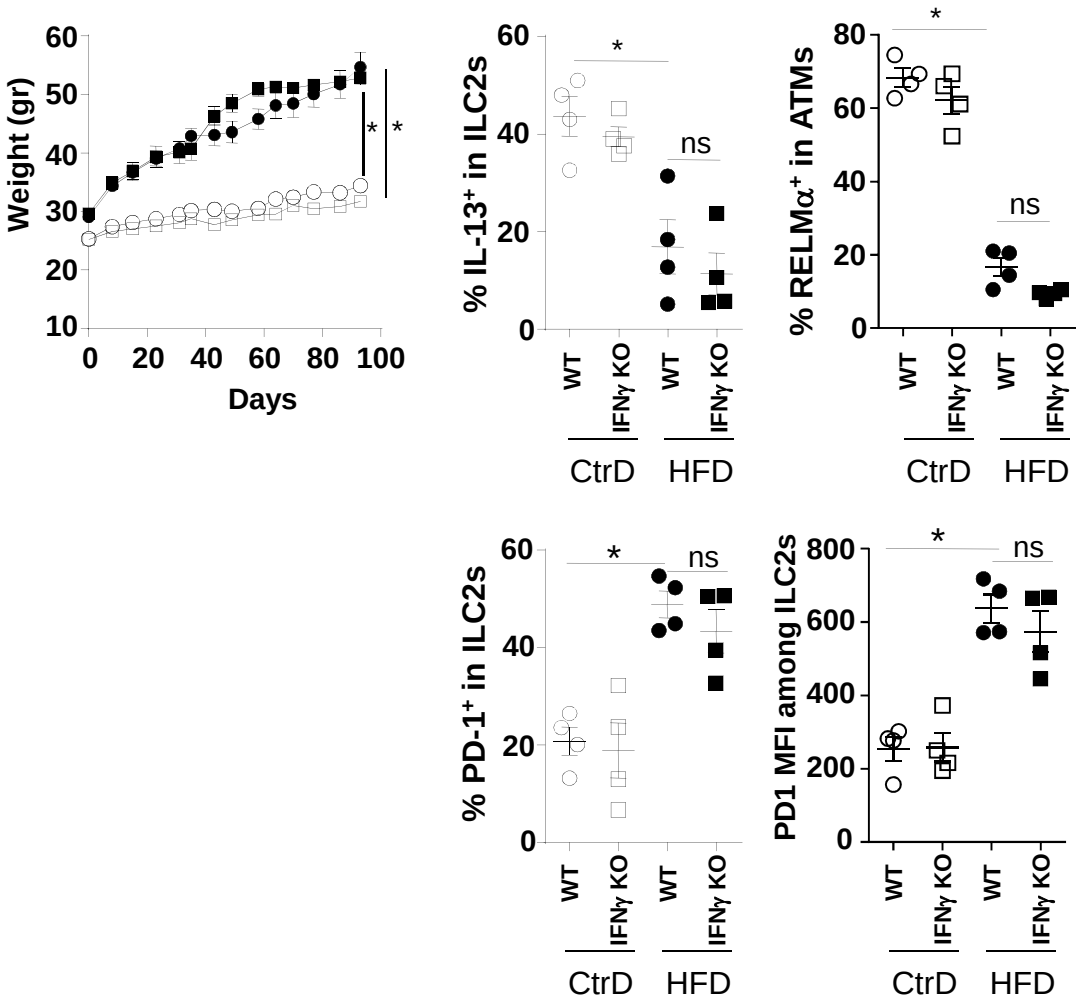

Supplemental Figure 3: Role of IFN-γ in ILC2 function during obesity; related to figure1. 8 wk old males C57BL/6 WT and IFN-γ KO were fed HFD or CtrD for 12 weeks. The weights were measured weekly and the stromal vascular fraction was extracted from the visceral adipose tissue.

Cells were stimulated shortly *in vitro* with PMA/ionomycin in the presence of brefeldin A and the ILC2s (defined as CD90.2$^+$ lin$^-$ Sca1$^+$ CD25$^+$ ST2$^+$) were analyzed by flow cytometry for their capacity to produce IL-13 (upper panels). Data are expressed as the percentage of IL-13$^+$ among ILC2s. The percentage of adipose tissue macrophages (ATMs; defined as MHCII$^+$ CD64$^+$ CD11b$^+$) expressing RELMα was determined by flow cytometry (upper right panel). ILC2s were analyzed by FACS for their expression of PD-1. Graphs illustrate the percentage of PD1$^+$ among ILC2s from WT and KO mice and the intensity of expression of PD-1 on ILC2s (lower panels).

Error bars represent the SDs of the means of 4 individual mice (*p <0.05, ns = not significant). Data are representative of 3 independent experiments with similar results.

Supplemental Figure 4:

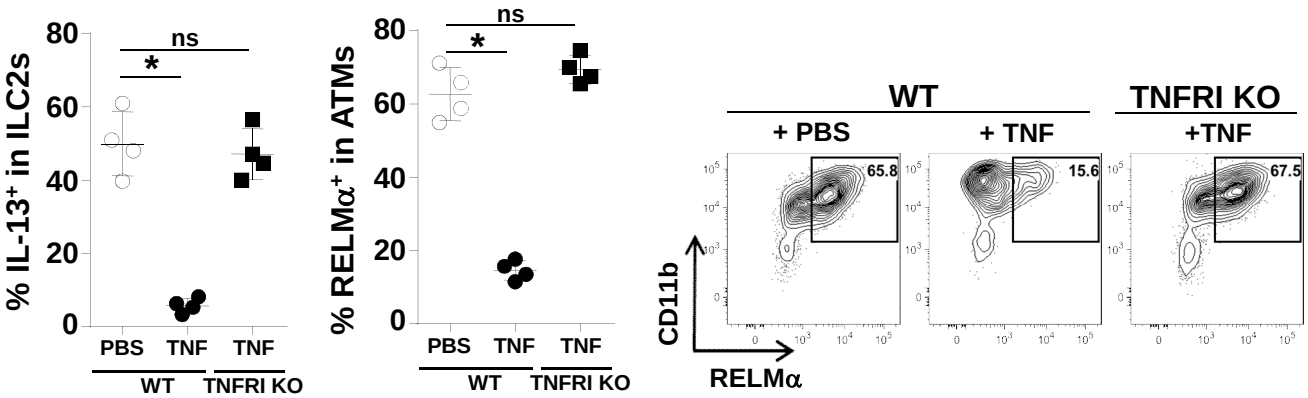

Supplemental Figure 4: ILC2 loss of function is dependent on the expression of TNFR1; related to figure 3. WT or TNFR1 KO mice were treated with recombinant TNF (2 intraperitoneal injections of 1µg at days 0 and 1). At day 2, the stromal vascular fraction was extracted from the visceral adipose tissue and cells were analyzed by flow cytometry. Cells were shortly restimulated with PMA-ionomycin in the presence of brefeldin A and ILC2s were analyzed for their intracellular IL-13 content. Comparative assessment of IL-13$^+$ ILC2 and RELMα$^+$ ATM frequencies in WT or TNFRI KO mice injected with TNF. Error bars represent the SDs of the means of 4 individual mice (*p <0.05, ns = not significant). Dot plots illustrate the expression of RELMα by CD11b$^+$ CD64$^+$ MHCII$^+$ ATMs. Numbers in quadrants refer to the percentage of CD11b$^+$ RELMα. Each dot plot is representative of one mouse. Data are representative of 3 independent experiments with similar results.

Table S1: Primers used in qRT-PCR
(Related to KEY RESOURCES TABLE in STAR METHODS)

REAGENT or RESOURCE	SOURCE	IDENTIFIER
Oligonucleotides		
RPL32-F: GGCACCAGTCAGACCGATAT	This paper	N/A
RPL32-R:'CAGGATCTGGCCCTTGAAC	This paper	N/A
IL13-F: AGGAGCTGAGCAACATCACA	This paper	N/A
IL13-R: CCAGGTCCACACTCCATACC	This paper	N/A
IL5-F: CATGAGCACAGTGGTGAAAGA	This paper	N/A
IL5-R: AAGCCTCATCGTCTCATTGC	This paper	N/A
UCP1-F: ACTGCCACACCTCCAGTCATT	This paper	N/A
UCP1-R: CTTTGCCTCACTCAGGATTGG	This paper	N/A
p40 F: GGAAGCACGGCAGCAGAATA	This paper	N/A
p40-R :AACTTGAGGGAGAAGTAGGAATGG	This paper	N/A
p35-F : CCTCAGTTTGGCCAGGGTC	This paper	N/A
p35-R : CAGGTTTCGGGACTGGCTAAG	This paper	N/A
iNOS-F : GCAACTACTGCTGGTGGTGA	This paper	N/A
iNOS-R : GGCTGGACTTTTCACTCTGC	This paper	N/A